Photodiagnosis and Photodynamic Therapy (2013) xxx, xxx–xxx

Available online at www.sciencedirect.com

SciVerse ScienceDirect

journal homepage: www.elsevier.com/locate/pdpdt

Photodynamic inactivation of *Staphylococcus aureus* and methicillin-resistant *Staphylococcus aureus* with Ru(II)-based type I/type II photosensitizers

Yaxal Arenas[a], Susan Monro[b], Ge Shi[b], Arkady Mandel[a], Sherri McFarland[b,*], Lothar Lilge[c,*]

[a] *Theralase Technologies, 1945 Queen St. East, Toronto, ON M4L 1H7, Canada*
[b] *Acadia University, 6 University Ave., Wolfville, NS B4P 2R6, Canada*
[c] *Princess Margaret Cancer Institute/University of Toronto, Department of Medical Biophysics, 610 University Ave., Toronto, ON M5G 2M9, Canada*

KEYWORDS
Photodynamic inactivation (PDI);
Photodynamic antimicrobial chemotherapy (PACT);
Antibiotic-resistant bacteria;
Ru-based photosensitizers;
Staphylococcus aureus;
Methicillin-resistant *Staphylococcus aureus*;
Sterilization;
Nosocomial infection

Summary
Background: The introduction of new disinfection and sterilization methods, such as antimicrobial photodynamic therapy, is urgently needed for the healthcare industry, in particular to address the pervasive problem of antibiotic resistance. This study evaluated the efficacy and the mechanisms of photodynamic antimicrobial chemotherapy (PACT), also known as photodynamic inactivation (PDI) of microorganisms, induced by novel Ru(II)-based photosensitizers against *Staphylococcus aureus* and methicillin-resistant *S. aureus* strains.
Methods: The photodynamic antibacterial effects of a new class of Ru(II)-based photosensitizers (TLD1411 and TLD1433) were evaluated against a strain of *S. aureus* (ATCC 25923) and a methicillin-resistant strain of *S. aureus* (MRSA, ATCC 33592). Bacterial samples were dosed with a range of photosensitizer concentrations (0.3–12 μM) and exposed to 530 nm light (90 J cm^{-2}) in normoxic conditions (ambient atmosphere) and in hypoxic conditions (0.5% O_2).
Results: Both photosensitizers exerted photodynamic inactivation (PDI) of the microorganisms in normoxia, and this activity was observed in the nanomolar regime. TLD1411 and TLD1433 maintained this PDI potency under hypoxic conditions, with TLD1433 becoming even more active in the low-oxygen environment.
Conclusion: The observation of activity in hypoxia suggests that there exists an oxygen-independent, Type I photoprocess for this new class of compounds in addition to the typical Type II pathway mediated by singlet oxygen. The intrinsic positive charge of the Ru(II) metal

* Corresponding authors.
E-mail addresses: yarenas@theralase.com (Y. Arenas), 053189m@acadiau.ca (S. Monro), 081973s@acadiau.ca (G. Shi), amandel@theralase.com (A. Mandel), sherri.mcfarland@acadiau.ca (S. McFarland), llilge@uhnres.utoronto.ca (L. Lilge).

1572-1000/$ – see front matter
http://dx.doi.org/10.1016/j.pdpdt.2013.07.001

Please cite this article in press as: Arenas Y, et al. Photodynamic inactivation of *Staphylococcus aureus* and methicillin-resistant *Staphylococcus aureus* with Ru(II)-based type I/type II photosensitizers. Photodiagnosis and Photodynamic Therapy (2013), http://dx.doi.org/10.1016/j.pdpdt.2013.07.001

combined with the oxygen independent activity demonstrated by this class of photosensitizers presents a new strategy for eradicating both gram-positive and gram-negative bacteria regardless of oxygenation level.

Introduction

The need for new strategies to combat antimicrobial-resistant microorganisms is an urgent one. *Staphylococcus aureus* in particular is a versatile opportunistic pathogen that is responsible for a wide variety of conditions, ranging from superficial skin infections to severe, invasive diseases [1,2]. Once treatable with penicillin regardless of strain, now many of its strains are resistant to beta-lactams, macrolides, and even vancomycin [3], the ''drug of last resort''. Methicillin-resistant (MRSA) and vancomycin-resistant *S. aureus* (VRSA) are collectively recognized as a very serious health threat, representing a major cause of mortality and adding financial burden to already-stretched health care systems [4]. Hence, there is significant practical, clinical, and commercial incentive to explore novel approaches to treating bacterial infection, not simply relying on the one drug, one site of action model characteristic of traditional antibiotics. Photodynamic inactivation (PDI) of pathogenic bacteria, also referred to as photodynamic antimicrobial chemotherapy (PACT) or antimicrobial photodynamic therapy (aPDT), is one such approach and is specifically unique in that it has not been shown to be susceptible to antibiotic resistance [5–7].

PDI in the conventional approach combines a photosensitizing drug (PS) and light to generate cytotoxic singlet oxygen and other reactive oxygen species (ROS). This oxidative burst leads to nonspecific damage with multi-faceted targets, including the cytoplasmic membrane, intracellular proteins, and DNA. Theoretical levels of cytotoxic substances released can reach up to 10^{12} M during light exposure [8]. Given that the $^1O_2$ rate of production is 10^6 to 10^8 s^{-1} for most PS and that the $^1O_2$ produced per PS molecule is typically 10^4, bacteria are simply not equipped with the antioxidant capacity required to combat an attack of this magnitude. Accordingly, antibiotic resistance to PDI is unlikely and has not been reported [9].

Numerous organic PSs have been probed for their potential to destroy pathogenic bacteria, including halogenated xanthenes (Rose Bengal), phenothiazines (Toluidine Blue, Methylene Blue), conjugated macrocycles such as acridines, phthalocyanines and porphyrins, and natural products such as hypericin [10]. While these neutral and anionic organic PS readily inactivate gram-positive microorganisms, targeting the more elusive gram-negative bacteria (e.g., *E. coli*) remains a challenge. Recently, cationic PS, including some Ru(II) complexes, were demonstrated to possess the ability to inactivate gram-negative species.[11] Current thinking is that the cationic PS benefits from enhanced binding through electrostatic interactions with the negatively charged outer membrane of gram-negative bacteria that exclude neutral and anionic PS. Thus, increased membrane-penetration of the cationic PS ensures that photogenerated singlet oxygen elicits its ascribed deleterious intracellular effect toward the microbe. This example, nicely illustrated by a Ru(II) complex of the type $[Ru(bpy)_2(dppn)]^{2+}$, relies on the intrinsic positive charge of the Ru(II) metal and a high singlet oxygen quantum yield for its acute activity. Consequently, an oxygenated environment is necessary for this mechanism of action that is not characteristic of all pathogenic targets. For instance, partial anaerobes such as MRSA thrive in hypoxia [12]. Therefore, new strategies for PDI that unite the attractive features of cationic Ru(II) complexes with oxygen-independent, Type I photoprocess will prove invaluable in constructing a complete arsenal of PDI agents for both aerobic and anaerobic conditions.

Herein we report a class of potent Type I/Type II Ru(II)-based PDI agents (Fig. 1) and validate their activity against MRSA, a pathogenic species chosen specifically because it is able to survive and grow in conditions irrespective of oxygen tension [12]. Compared to their organic counterparts, Ru(II) coordination complexes are known for their unusual chemical and photochemical stabilities, structurally modular design, and rich photophysical and photochemical properties. Still, it remains a difficult challenge to instill Type I photochemical activity into such structures and even more so in organic PSs. The Ru(II)-based PSs in this report can generate singlet oxygen with close to 100% efficiency but have the capacity to switch to a Type I mechanism in hypoxic environments. This ability to mediate photoinduced electron transfer reactions directly opens up the possibility of targeting microorganisms with PDI in hypoxic environments.

Materials and methods

General

S. aureus (ATCC 25923, Cedarlane, Canada) and methicillin-resistant *S. aureus* (MRSA, ATCC 33592, Cedarlane, Canada), were grown overnight at 37 °C in Columbia media (BD, Canada) either in aerobic or hypoxic atmospheric conditions as described below. Columbia agar plates were used to grow colonies of *S. aureus*, whereas oxacillin-resistance agar plates (Oxoid, Canada) were required for MRSA CFU counting. Methylene blue (MB), thioglicolate, resazurin, bovine serum albumin (BSA) and synthetic reagents for the preparation of TLD1411 and TLD1433 were purchased from Sigma Aldrich (Canada). Solvents were purchased from Fisher Scientific (Canada). Silica gel was purchased from Silicycle (Canada), Amberlite IRA-410 was purchased from Fluka (Canada), and deuterated solvents for NMR spectroscopy were obtained from Caledon (Toronto, ON, Canada).

Instrumentation

NMR spectra were collected using a 300 MHz Bruker BZH 300/52 spectrometer at Acadia's Center for Microstructural Analysis and a Bruker AV 500 MHz Spectrometer at The Nuclear Magnetic Resonance Research Resource at Dalhousie

Please cite this article in press as: Arenas Y, et al. Photodynamic inactivation of *Staphylococcus aureus* and methicillin-resistant *Staphylococcus aureus* with Ru(II)-based type I/type II photosensitizers. Photodiagnosis and Photodynamic Therapy (2013), http://dx.doi.org/10.1016/j.pdpdt.2013.07.001

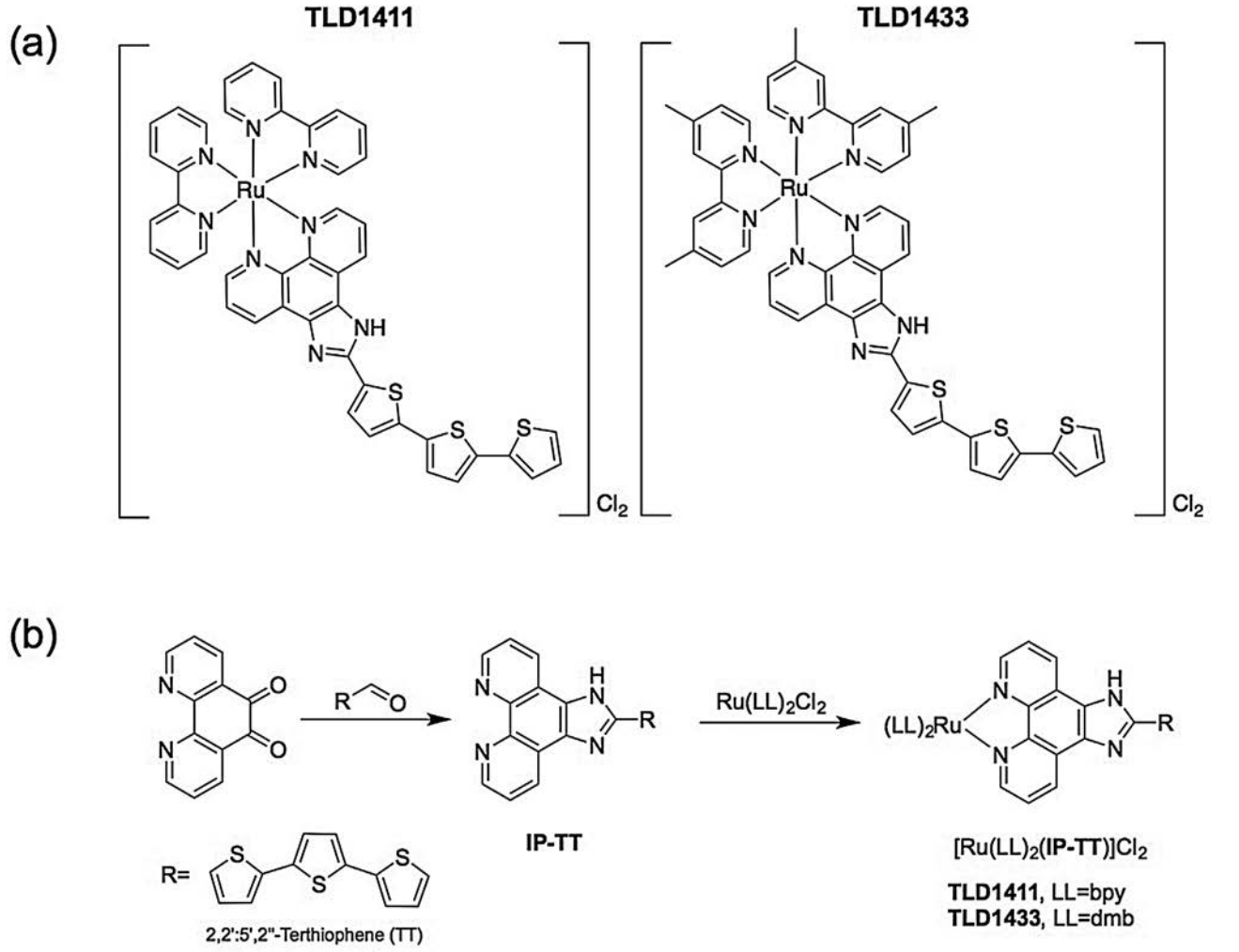

Fig. 1 (a) Chemical structures of TLD1411 and TLD1433, PS used in this study; (b) general synthetic scheme for the preparation of IP-TT and its complexation to form TLD1411 and TLD1433, respectively.

University. ESI-MS spectra were obtained using a Bruker microTOF Focus Mass Spectrometer from the Maritime Mass Spectrometry Laboratories at Dalhousie University. Elemental analysis was obtained from Canadian Microanalytical Service Ltd (Delta, BC, Canada). UV—Vis spectra were collected using a Jasco V-530 (Easton, MD, US) spectrophotometer. Emission spectra were collected using a custom built version of PTI's QuantaMaster (London, ON, Canada) equipped with a Red-PMT and a Hamamatsu NIR PMT for measuring singlet oxygen quantum yields directly. Photobleaching experiments were carried out using Varian's Cary 300 Bio UV-visible absorption spectrometer (Agilent Technologies, Mississauga, Canada), and high-throughput colorimetric assays were performed on a SpectraMax M5 plate reader (Molecular Devices, Sunnyvale, USA) in fluorescence mode (λ_{ex} = 570 nm, λ_{em} = 600 nm) following a protocol established in-house [13]. A high-power LED, manufactured by Theralase, Inc. (Toronto, ON, Canada) (530 ± 25 nm) with an average irradiance of 98 ± 2 mW cm^{-2} served as the primary light source for all PDI experiments, and the light source used for photobleaching measurements was a 532 nm-laser (Verdi-5W, Coherent Santa Clara, USA).

Synthesis

[1,10]phenanthroline-5,6-dione [1,10]. Phenanthroline monohydrate (1.00 g, 5.04 mmol) was combined with KBr (5.95 g, 50 mmol) in a 100 mL round bottom flask and immersed in an ice bath. Concentrated H_2SO_4 (20 mL) was added drop wise down the side of the flask, followed by concentrated HNO3 (10 mL). The resulting solution was warmed to room temperature and then heated at 80—85 °C for 2 h. The reaction mixture was subsequently cooled to room temperature and added to 400 mL deionized H_2O, resulting in a yellow solution that was made slightly basic through the addition of a saturated $NaHCO_3$. The product was extracted into dichloromethane, dried over $MgSO_4$, and concentrated under reduced pressure to give a yellow solid. (0.635 g, 60%). Rf = 0.73 (2% H_2O, 43% $CHCl_3$, 25% Acetone, 30% MeOH + 1% NH_4OH (v/v)). 1H NMR ($CDCl_3$) δ 7.63 (dd, 2H, b-H), 8.55 (dd, 2H, c-H), 9.16 (dd, 2H, a-H).

2-(2′,2″:5″,2‴-terthiophene)-imidazo[4,5-f][1,10] phenanthroline (IP-TT). 1,10-Phenanthroline-5,6-dione (166.6 mg, 0.800 mmol), ammonium acetate (616 mg, 8.00 mmol), and 5-formyl-2,2′:5′,2″-terthiophene (221.12 mg,

Please cite this article in press as: Arenas Y, et al. Photodynamic inactivation of *Staphylococcus aureus* and methicillin-resistant *Staphylococcus aureus* with Ru(II)-based type I/type II photosensitizers. Photodiagnosis and Photodynamic Therapy (2013), http://dx.doi.org/10.1016/j.pdpdt.2013.07.001

0.800 mmol) were combined with glacial acetic acid (4.0 mL) in a microwave reaction chamber and reacted (300 W, 180 °C) for 10 min. The deep red solution was cooled to room temperature and neutralized by drop-wise addition of aqueous NH_4OH until the product precipitated as a yellow/brown solid. The solid was collected using a fine glass-sintered frit and washed with H_2O. The product was dried under vacuum to give a tan powder in 70% yield. Rf = (2% H_2O, 43% $CHCl_3$, 25% Acetone, 30% MeOH + 1% NH_4OH). 1H NMR (DMSO-d_6) 8.97 (d; 2H; J = 3.00 Hz; 6, 9), 8.82 (d; 2H; J = 8.01 Hz; 4, 11), 7.75—7.79 (m; 3H; 5, 10, 4′), 7.55 (m; 1H; 5‴), 7.33—7.43 (m; 4H; 3, 3″, 4″, and 3‴), 7.14 (dd; 1H; J = 4.37 Hz; 4‴).

$Ru(LL)_2Cl_2{\cdot}2H_2O$ (LL = bpy, dmb) [14] $RuCl_3{\cdot}3H_2O$ (1.155 g, 4.4 mmol), 2,2′-bipyridine (bpy) or 4,4′-dimethyl-2,2′-bipyridine (dmb) (1.5 g or 1.8 g, respectively, 9.6 mmol), LiCl (2.9 g, 68.5 mmol) and 10 mL DMF were placed in a flask and heated to 160 °C with stirring overnight. The mixture was cooled to room temperature and transferred to a beaker where 50 mL of acetone was added. The beaker was placed in a freezer at −10 to 0 °C for 2 h, then the flask was removed and allowed to warm to room temperature. The mixture was filtered and washed with water until the filtrate ran clear (>200 mL) and finally with diethyl ether (3—4 mL). The product was dried under vacuum for 2 h to afford a black product in accordance with published data.

TLD1411. $Ru(bpy)_2Cl_2{\cdot}2H_2O$ and IP-TP were combined in an equimolar ratio in absolute ethanol under an argon atmosphere. The solution was reacted (300 W, 180 °C for 10 min in a Discover microwave single-vessel reactor to yield a deep, dark red solution. Saturated KPF_6 was added drop-wise to the ethanolic solution until no additional product precipitated. The crude product was isolated by filtration through a fine glass-sintered frit yielding a bright red/orange solid. Purification was done on a silica column, eluting with a 10% H_2O:MeCN solution containing 2.5% KNO_3, and the principle red spot was collected (Rf = 0.46). The fractions containing the desired product were combined, evaporated under reduced pressure, and further dried under vacuum to give the corresponding NO_3^- complex and excess KNO_3. To remove the unwanted salt, the product was dissolved in H_2O with sonication. Saturated KPF_6 was added, and the product precipitated out of solution. The desired PF_6^- complex was extracted using CH_2Cl_2. The organic layer was separated, concentrated under reduced pressure, and dried under vacuum to give the final pure product as a red-orange solid in approximately 50% yield. Rf = 0.41 (10% H_2O:MeCN + 2.5% KNO_3). ^1H NMR (CD_3CN): 8.65 (d; 2H; J = 7.89 Hz; C), 8.51—8.55 (m; 4H; 3, 3′), 7.96—8.11 (m; 6H; 4), 7.85 (d; 2H; J = 5.49 Hz; 6′), 7.72 (d; 1H; J = 3.81 Hz; E), 7.61—7.67 (m; 4H; B, 6), 7.46 (t; 2H; J = 6.93 Hz; 6′), 7.37 (d; 1H; J = 5.10 Hz; K), 7.06—7.30 (m; 7H; 5, D, F, G, I, J). MS (ESI+) *m/z*: 440.0 $[M\text{-}2PF_6]^{2+}$, 879.1 $[M\text{-}2PF_6{}^-1H]^+$. HRMS (ESI+) *m/z* for $C_{45}H_{30}N_8RuS_3$; calc. 440.0399; found 440.0382. The PF_6^- complex was dissolved in a 1:1 solution of MeCN/MeOH and converted to its corresponding Cl^- salt on Amberlite IRA-410 ion exchange resin (30 cm × 1.5 cm, 30 g of resin) eluting with MeOH. Anal. Calc. $C_{45}H_{30}Cl_2N_8RuS_3 \cdot 4.065(H_2O)$: C, 52.77%; H, 3.75%; N, 10.94%, Found: C, 51.78%; H, 4.25%; N, 10.20%.

TLD1433. $Ru(dmb)_2Cl_2{\cdot}2H_2O$ and IP-TP were combined in equimolar ratios in absolute ethanol in a microwave tube under argon. The solution was irradiated (300 W, 180 °C for 10 min in the Discover single-vessel microwave reactor. To the resulting deep, dark red solution, saturated KPF_6 was added drop-wise until no additional product precipitated. The crude product was isolated by filtration through a fine glass-sintered frit to give a red/brown solid. Purification was done on a silica column, eluting with a 10% H_2O:MeCN solution containing 2.5% KNO_3, and the principle red spot was collected (Rf = 0.54). The fractions containing the desired product were combined, evaporated under reduced pressure, and further dried under vacuum to give the corresponding NO_3^- complex and excess KNO_3. To remove the unwanted salt, the product was dissolved in H_2O with sonication. Saturated KPF_6 was added to precipitate the product. The desired PF_6^- complex was extracted using CH_2Cl_2, and the organic layer was separated, concentrated under reduced pressure, and dried under vacuum to give the final pure product as a red-orange solid in approximately 60% yield. Rf = 0.54 (10% H_2O:MeCN + 2.5% KNO_3). ^1H NMR (CD_3CN): 8.87 (d; 2H; J = 6.60 Hz; C), 8.38 (d; 4H; J = 10.1 Hz; 3, 3′), 8.02 (m; 2H; J = 4.50 Hz; A), 7.84 (d; 2H; J = 4.02 Hz; E), 7.74 (br; 2H; B), 7.67 (d; 2H; J = 5.67 Hz; 6′), 7.53 (d; 1H; J = 6.42 Hz; K), 7.42 (d; 2H; J = 5.67 Hz; 6), 7.25—7.31 (m; 6H; 5′, D, F, G, I), 7.07—7.14 (m; 3H; 5, J). MS (ESI+) *m/z*: 468.1 $[M\text{-}2PF_6]^{2+}$, 1081.2 $[M\text{-}PF_6]^+$. HRMS (ESI+) *m/z* for $C_{49}H_{38}N_8RuS_3$; calc. 468.0707; found 468.0697. The PF_6^- complex was dissolved in a 1:1 solution of MeCN/MeOH and converted to its corresponding Cl^- salt on Amberlite IRA-410 ion exchange resin (30 cm × 1.5 cm, 30 g of resin) eluting with MeOH.

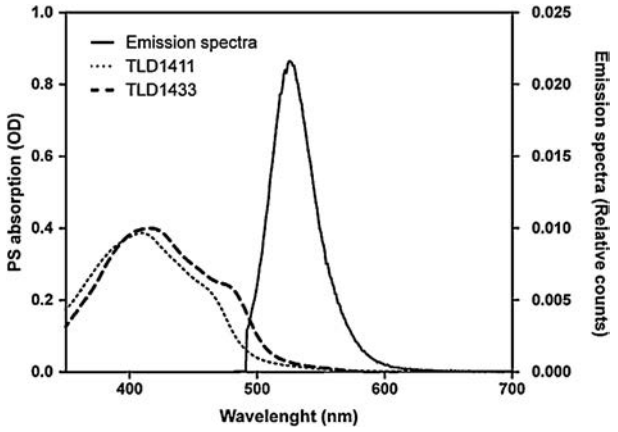

Fig. 2 Normalized absorption spectra of PS TLD1411 and TLD1433 and normalized emission spectra of the light source.

Photobleaching

Photobleaching by each PS was quantified by changes in the UV—Vis absorption spectroscopic signature at 425 nm (Figs. 2—3). Aqueous samples of PS were exposed to 525 nm irradiation at 200 mW cm^{-2} and measured in 5 min intervals for a total of 60 min. The OD was recorded using a dual-beam spectrophotometer set to OD 413 nm to increase sensitivity to absorbance changes. The reference solvent in the OD measurements was either water or BSA (25 μM for TLD1411, and 33.5 μM for TLD1433), where BSA was used to simulate PDI conditions more realistically [8]. Photobleaching as a

Please cite this article in press as: Arenas Y, et al. Photodynamic inactivation of *Staphylococcus aureus* and methicillin-resistant *Staphylococcus aureus* with Ru(II)-based type I/type II photosensitizers. Photodiagnosis and Photodynamic Therapy (2013), http://dx.doi.org/10.1016/j.pdpdt.2013.07.001

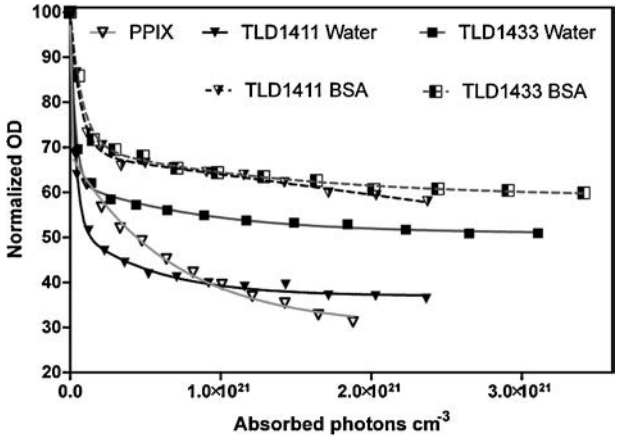

Fig. 3 Photobleaching of PPIX (1.3 uM in DMSO), TLD1411 (5 μM) and TLD1433 (6.7 μM), PPIX (1.3 μM) measured at 425 nm (normoxia) in water and in BSA, (25 μM, 33.5 μM) respectively, using the light source employed for PDI (530 nm).

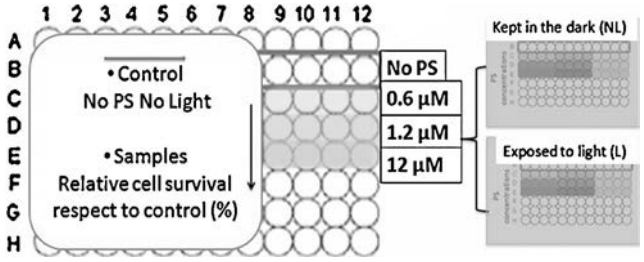

Fig. 4 Layout of the 96-well plate used for PDI.

function of the absorbed photon dose was calculated using GraphPad Prism software (La Jolla, CA, USA).

PDI under normoxia

Cultures were grown overnight in Columbia broth. Bacterial reference aliquots were prepared by a dilution of the overnight culture in fresh media with an $OD_{\lambda=600\,nm}$ of 0.3, which is equivalent to 10^8 cfu mL^{-1}.[15] PS stock solutions of 2 mM were prepared in purified water (MilliQ, 18.5 mΩ), and serial dilutions were prepared in low light conditions to achieve final concentrations ranging from 12 to 0.03 μM. Fig. 4 shows the layout on a typical 96-well plate along with a timeline for the experiment in Fig. 5. Bacterial aliquots were added to a 96 well plate (60 μL per well) followed by 60 μL of media with the appropriate PS dilution, including controls for each SA strain without PS. Plates were prepared in duplicate, whereby one plate served as a dark control and was incubated for 30 min with the PS in the dark at 37 °C. The other plate with identical bacteria and PS concentrations was exposed to light for 10 min (total radiance exposure of 58.8 J cm^{-2}). Bacterial quantification was carried out using a modified Alamar Blue assay [13] and also by manual counting. The colorimetric assay relied on the well-known ability of metabolically active cells to reduce nonfluorescing reazurin to resorufin. The number of bacteria (BC) was extrapolated through a series of exponential fits adjusted to the slopes (SKRA) of a series of kinetic fluorescent measurements, bacterial strain and environmental conditions determine according to Eq. (1), where parameters *a* and *b* are specific to a bacterial strain and environmental conditions and represent the initial slope and the maximum signal at long times, respectively.

$$BC = a \times 10^7 e^{SKRT/b} \quad (1)$$

For manual counting, 20 μL aliquots diluted in PBS were plated on Columbia agar plates, and colonies were counted after 24-h incubation at 37 °C.

PDI under hypoxia

In order to create hypoxic conditions, two 5-L bags of Anaerogen (Oxoid, Canada) were placed in an environmental chamber, and a mixture of 0.5% CO_2 in N_2 (Praxair, Toronto, Canada) was introduced for 30 min to consume residual oxygen. All liquid reagents, including media and water, were also sparged with 0.5% CO_2 in N_2. A mixture of sodium thioglycolate (0.68 μM) and resazurin (17.45 μM) was added to the media before mixing with bacteria to ensure maximum realistic oxygen consumption. Glass tubes with rubber stoppers were used to preserve hypoxic conditions during bacterial incubation prior to PDT light exposure. To further minimize O_2, all tools and plastic dishes were kept in the chamber at 0.5% O_2,/5% CO_2-balanced N_2 for 12 h before experiments were started. Subsequent PDI procedures were performed as described for normoxic conditions inside the hypoxic chamber. The CFU assay was the standard method used to recover bacterial survival number after PDI treatment; no colorimetric assay was used (Fig. 6).

Singlet oxygen quantum yields

PS solutions were prepared in acetonitrile at 5 μM, with OD < 0.05 at their longest wavelength absorption maxima. Excitation and emission were carried out using the PTI QuantaMaster equipped with a NIR detector, exciting the lowest energy metal-ligant charge transition (MLCT) and collecting direct emission from singlet oxygen between 1200—1350 nm

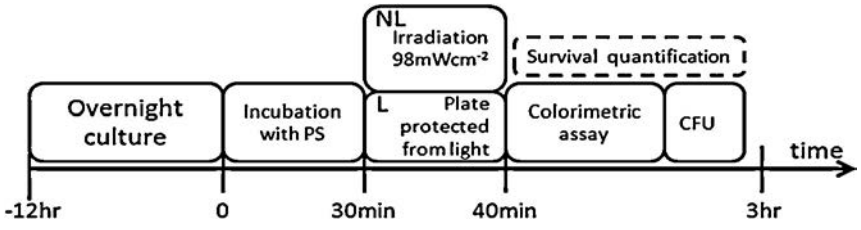

Fig. 5 Experimental timeline for PDI in normoxia.

Please cite this article in press as: Arenas Y, et al. Photodynamic inactivation of *Staphylococcus aureus* and methicillin-resistant *Staphylococcus aureus* with Ru(II)-based type I/type II photosensitizers. Photodiagnosis and Photodynamic Therapy (2013), http://dx.doi.org/10.1016/j.pdpdt.2013.07.001

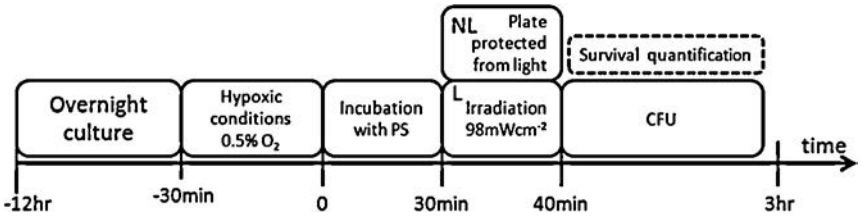

Fig. 6 Experimental timeline for PDI in hypoxia.

using a 1000-nm long-pass filter to remove scattered photons from the excitation source. $[Ru(bpy)_3]^{2+}$ was used as the standard, which has a known singlet oxygen quantum yield of 0.56 in acetonitrile [16]. Relative quantum yields were calculated according to standard methods [17].

Emission quantum yields

Samples of PS were prepared as indicated in the previous section, excited at their longest wavelength absorption maxima, and monitored using PDT's QuantaMaster equipped with a Red-PMT. Emission was collected between 575—900 nm in aerated acetonitrile with a 525-nm long pass filter in place to remove stray light. $[Ru(bpy)_3]^{2+}$ was used as the standard, which has a known emission quantum yield of 0.012 in aerated acetonitrile [18]. Relative quantum yields were calculated in the same manner as for singlet oxygen.

Results

Synthesis and characterization

TLD1411 and TLD1433 were synthesized according to a modification of standard procedures [19] for assembling heteroleptic Ru(II) complexes of the type $[Ru(LL)_2(LL')]^{2+}$, where LL is a diimine ligand that lends stability to the overall pseudo-octahedral coordination sphere and LL′ is a photoactive ligand that is tailored to impart unique photophysical and photochemical properties to the overall complex (Fig. 1). The complexes were prepared using microwave irradiation (300 W, 180 °C), which significantly reduced reaction times. A similar modification was used to synthesize LL′, originally prepared by Batista et al. [20] according to conventional methods, in excellent yield. Complexation of 2-(2′,2″:5″,2‴-terthiophene)-imidazo[4,5-f] [1,10]phenanthroline (LL′), with either $Ru(bpy)_2Cl_2$ or $Ru(dmb)_2Cl_2$ gave TLD1411 and TLD1433 in 50% yield and 60% yield after purification, respectively.

Structural confirmation of TLD1411 and TLD1433 was provided by ESI mass spectrometry, ^{1}H NMR spectroscopy, and elemental analysis. Of importance to this work, UV—Vis absorption spectroscopy (Fig. 2) revealed typical ^{1}LC and ^{1}MLCT transitions characteristic of Ru(II) coordination complexes, with longest wavelength absorption maxima near 420 nm and no significant absorption past 575 nm [21,22]. Regardless of excitation wavelength, these PSs were virtually nonemissive in all solvents with aerated luminescence quantum yields less than 0.05%, further supported by quantum yields for singlet oxygen production approaching unity [23]. In deoxygenated solution, the emission quantum yield for TLD1411 barely approached 0.1%, with TLD1433 only 0.05%. This poor emission of both PSs in the absence of oxygen signals the presence of an alternate excited state relaxation pathway that is very efficient in this class of PSs and is crucial to retaining PDI in hypoxia.

Photobleaching

The ability of a PS to resist photobleaching is an important consideration in choosing an agent for PDI, and cationic Ru(II) complexes in particular are renowned for their excellent photostability. Photobleaching, or the degradation of a PS with prolonged light exposure, can significantly reduce the potency of PDI. PPIX, a gold standard in terms of Type II agents for PDI, was tested under the same conditions as the TLD1400 series and showed a 55% reduction in its absorption coefficient after 6.4×10^{14} absorbed photons per cm^{-3}, which culminated in a 70% overall reduction at 1.8×10^{21} absorbed photons per cm^{-3} (OD measured at 411 nm). By comparison TLD1411 and TLD1433 were bleached by only 25% and 23%, respectively, in the first 2.7×10^{19} absorbed photons per cm^{-3} (Fig. 3). Overall, TLD1411 and TLD1433 were bleached by 49% and 63%, with TLD1411 being slightly more susceptible to photobleaching in water. Importantly, when PDI conditions were simulated with the addition of a 1.25 fold excess of BSA, the biphasic bleaching curves of of TLD1411 and TLD1433 were almost super imposable (average 10% loss, $P < 0.0001$ in a 2-tailed ANOVA). Notably, the TLD1400 series was bleached by only about 35% overall in BSA solution, suggesting a high resistance to bleaching during PDI in comparison to clinical agents such as PPIX.

PDI

Two independently prepared batches of TLD1411 and TLD1433 were synthesized to ensure reproducibility of the photobiological activity of each PS. There were no differences in the absorption spectra or sterilization efficacy between the two batches of each PS. In *S. aureus*, the dark toxicity associated with TLD1433 increased with PS concentration while that for TLD1411 was independent of PS concentration in normoxia (average 1.2 logs of kill, Fig. 7, top left). In hypoxia, however, the dark toxicity of both TLD1411 and TLD1433 increased exponentially as a function of PS concentration (Fig. 7, bottom). Due to the concentration independence of the dark toxicity under normoxia for TLD1411, the PDI effect for TLD1411 in normoxia increased with increasing concentration to yield over 6 logs of difference between dark and light treatment at 12 μM PS. Notably, as little as 30 nM of PS induced a significant PDI effect for both TLD1411 and TLD1433 regardless of oxygenation conditions.

Please cite this article in press as: Arenas Y, et al. Photodynamic inactivation of *Staphylococcus aureus* and methicillin-resistant *Staphylococcus aureus* with Ru(II)-based type I/type II photosensitizers. Photodiagnosis and Photodynamic Therapy (2013), http://dx.doi.org/10.1016/j.pdpdt.2013.07.001

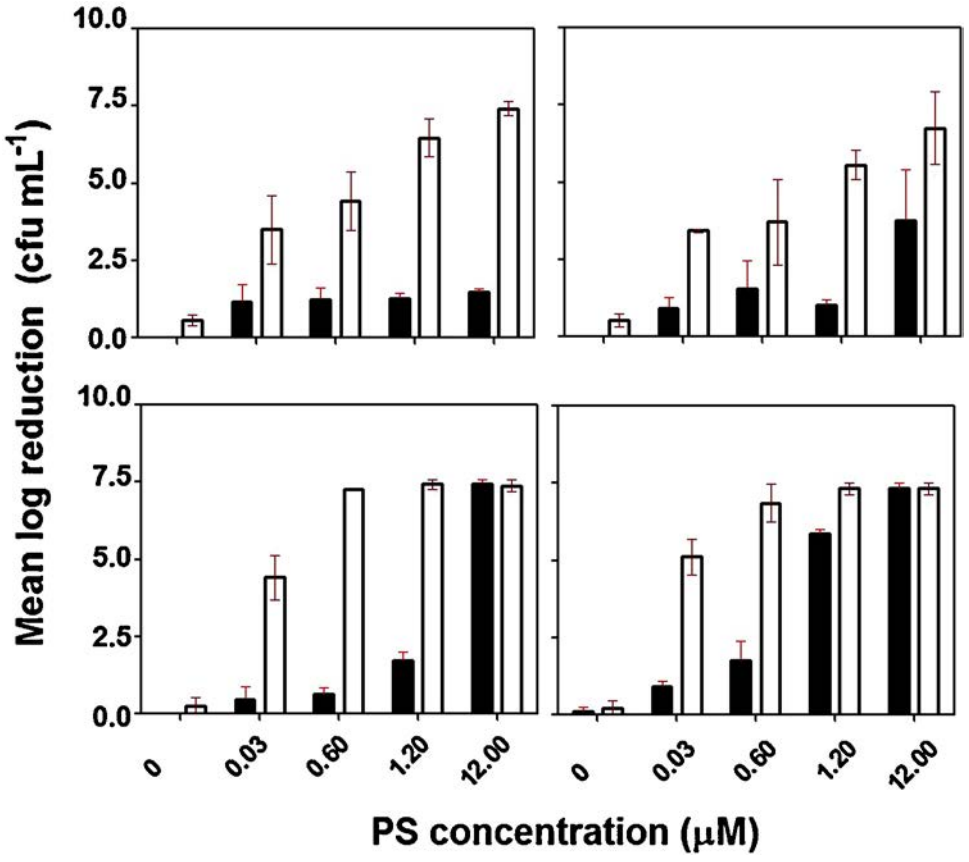

Fig. 7 Bactericidal activity of TLD1411 (left) and TLD1433 (right) against *S. aureus* in normoxia (top) and hypoxia (bottom). Dark toxicity: solid bars; light toxicity: open bars. Each bar is the average of 3 replicates with error bars indicated.

Overall, TLD1411 and TLD1433 were virtually nontoxic against MRSA in the dark (<1 log of kill) in comparison to *S. aureus*, leading to a much stronger PDI effect against MRSA (Fig. 8), albeit at 12 μM a critical concentration appears to be reached showing variability in the dark toxicity between experiments. The particular reason for this variability are not clear at this time. As for *S. aureus*, nanomolar PDI is evident in both normoxia and hypoxia, with the effect being as large as 7.5-log fold in the non-resistant strain. Unlike *S. aureus*, the PDI effect was not diminished to any extent in hypoxia. A summary of the photosensitized sterilization induced by TLD1411 and TLD1433 is presented in Table 1 for comparison. The TLD1400 series yielded photosensitized $\log_{10}$ reductions at their most effective concentrations no lower than 6.7 in all conditions, against *S. aureus* or MRSA in normoxia or hypoxia. The average light-induced $\log_{10}$ reduction across all conditions for both PSs was 7.26, with the highest reduction in microbial load occurring for TLD1433 against MRSA in normoxia ($\log_{10}$ reduction 8.5).

Table 1 Photosensitized inactivation, measured as $\log_{10}$ reductions, of *S. aureus* and MRSA by TLD1411 and TLD1433 in two atmospheric conditions.

	S. aureus		MRSA	
	Normoxic	Hypoxic	Normoxic	Hypoxic
TLD1411	7.4	7.5	6.9	7
TLD1433	6.7	6.8	8.3	7.5

As a way to investigate whether the TLD1400 series of PSs function as Type I agents, dark and light inactivation were tested in parallel with MB, a known Type II PS, under normoxia and hypoxia. As expected, treatment of *S. aureus* (and also MRSA) in hypoxia with MB resulted in no significant PDI effect at concentrations as high as 480 μM (Fig. 9). In contrast, the PDI efficacy of TLD1411 and TLD1433 against *S. aureus* in hypoxia was greater than that in normoxia at concentrations at or below 60 nM, similar in the low-micromolar range, and slightly less at 12 μM, where dark toxicity limits the PDI effect. Against MRSA, the PDI effect generated by TLD1411 in hypoxia was comparable at all concentrations to normoxia. Strikingly, TLD1433 demonstrated an increased PDI effect in hypoxia against MRSA at almost all concentrations employed. Notably, at the highest concentration included (12 μM) where PDI is not evident against MRSA in normoxia due to a higher baseline dark toxicity, TLD1433 showed a reduction difference between dark and light conditions of 4.7 $\log_{10}$ in hypoxia. It should be noted that at the concentration of the PS (0.03–12 μM) and light dose employed in these studies, MB was not effective against *S. aureus* or MRSA in normoxia or hypoxia. In fact, at least 60 μM MB was necessary to achieve a light-induced $\log_{10}$ reduction of over 3.5, and this occurred only in normoxia against *S. aureus*.

Please cite this article in press as: Arenas Y, et al. Photodynamic inactivation of *Staphylococcus aureus* and methicillin-resistant *Staphylococcus aureus* with Ru(II)-based type I/type II photosensitizers. Photodiagnosis and Photodynamic Therapy (2013), http://dx.doi.org/10.1016/j.pdpdt.2013.07.001

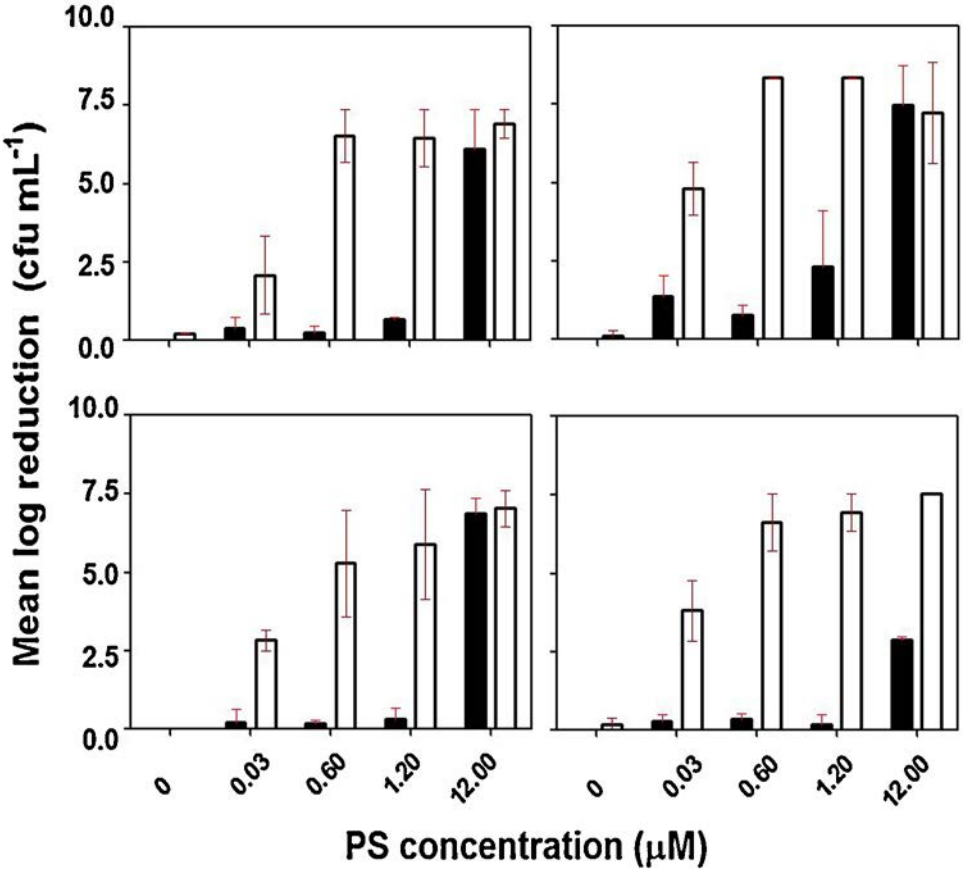

Fig. 8 Bactericidal activity of TLD1411 (left) and TLD1433 (right) against MRSA in normoxia (top) and hypoxia (bottom). Dark toxicity: solid bars; light toxicity: open bars. Each bar is the average of 3 replicates with error bars indicated.

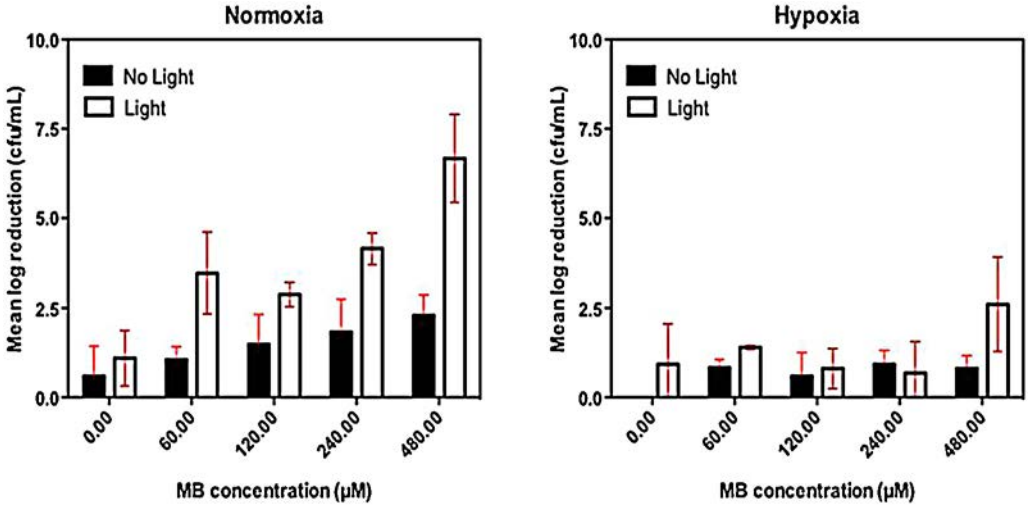

Fig. 9 Bactericidal activity of MB against *S. aureus* in normoxia and hypoxia. Dark toxicity: solid bars; light toxicity: open bars. Each bar is the average of 3 replicates with error bars indicated.

Discussion

While TLD1411 and TLD1433 have their highest-wavelength absorption maxima in the blue region of the spectrum, a 400-nm light source would be expected to have its intensity reduced by a factor of 50 in tissue applications [24]. Since both PSs absorb green light in measurable yields (log $\varepsilon = 3.17$ and 3.34, respectively), a 530-nm exciting light source was used in order to ensure up to 2-mm in penetration depth [25,26] for sterilization of bacteria inside tissue, e.g., infected wounds. In this scenario, the delivered light dose is expected to be reduced only to 37% of the incident radiant

Please cite this article in press as: Arenas Y, et al. Photodynamic inactivation of *Staphylococcus aureus* and methicillin-resistant *Staphylococcus aureus* with Ru(II)-based type I/type II photosensitizers. Photodiagnosis and Photodynamic Therapy (2013), http://dx.doi.org/10.1016/j.pdpdt.2013.07.001

exposure [27]. Because MB has been suggested as a PS for local disinfection (e.g., of wounds and ulcers) in the face of rampant rates of infection by MRSA [7], it was used as a reference compound in the present study. MB is approved for clinical use in a variety of capacities due to its low toxicity in humans, and as a PS specifically, it has shown effectiveness against gram-positive bacteria such as *S. aureus* and MRSA [28,29]. MB functions as a prototypical Type II PS, and in our conditions, as expected, MB photosensitizing activity was significantly diminished in hypoxia as demonstrated in Fig. 9 for *S. aureus*. It should be noted that not all traces of oxygen can be completely removed from the chamber, and this is exemplified by marginal PDI by MB at high concentration. However, Wang et al. [30] have shown that the effective $[^1O_2]$ is a function of the ratio $([^3O_2]/[^3O_2]+\beta)$, where β has been measured in the range of 11 μM for various PS. Hence, below 0.1 μM $^3O_2$, the ability to generate effective $^1O_2$ is reduced by two orders of magnitude. For example, the light toxicity of MB at the highest concentration employed (480 μM) in normoxia was 6.38 $\log_{10}$ reduction in microbial load while in hypoxia, microbial kill was only 2.91 $\log_{10}$ units which could have been achieved at a $[^3O_2]$ of 1 nM. Assuming similar dark toxicities under both conditions, MB was nearly 3000-fold less effective at low oxygen tension, supporting a primarily Type II photosensitization by MB. Two important points regarding the ensuing discussion are that (i) MB does not function as a Type I agent [31], and (ii) the concentrations of MB needed to achieve similar light kill to the TLD1400 series in both normoxia and hypoxia are up to 16,000-fold greater, and over 3 orders of magnitude for hypoxic conditions specifically. In other words, the TLD1400 class of PDI agents displays an unprecedented photodynamic effect against *S. aureus* and MRSA in the low-nanomolar regime, even under hypoxic conditions.

Equally important, the magnitude of photosensitized sterilization by the TLD1400 series is exceedingly large when comparison to other PS. Inactivation of MRSA by reported PDI agents ranges between 2 and 6 $\log_{10}$ reductions with standard light doses [32—34] whereas the best performer against MRSA in this study, TLD1433, produced an 8.3 $\log_{10}$ reduction in microbial load in normoxia (and was only reduced to 7.5 in hypoxia). Moreover, both PSs in all conditions (at their most effective concentrations) produced $\log_{10}$ reductions above 6.5, with the least effective condition (TLD1433 against *S. aureus*) still generating photosensitized microbial kill 5-fold greater than the best known PSs.

The differences in susceptibility of *S. aureus* and MRSA to PDI by the TLD1400 series was similar to what has been documented for other classes of photosensitizers. Kossakowska et al. [35] tested a range of *S. aureus* strains, finding MRSA more susceptible to PDI treatment by 1.1 to 1.8 $\log_{10}$ units for PPArg, TBO and ALA photosensitizers. Other studies show differences ranging from 0.04 to 1.69 $\log_{10}$ for $SnCe_6$ [36] and XF porphyrin derivatives [37]. Szpakowska et al. show a similar trend with a difference of 37.5 μM on the highest MIC value for MRSA compared to *S. aureus* [38]. It has been suggested that the increased PDI susceptibility of a given *S. aureus* or MRSA strain to a particular PS could be related to the ability of the PS to act as substrate for multidrug resistant pumps [39,40], in particular active efflux appears to be involved in staphylococcal responses to cationic antimicrobial substances. For example, the staphylococcal multidrug efflux pump QacA mediates resistance to a broad spectrum of monovalent and divalent antimicrobial cations [41]. The existence of efflux activity in *S. aureus* is strain dependent and could be more predominant in certain MRSA strains, such as HPV107. Hence, the efflux activity could link with a phenotype of reduced susceptibility toward several biocidal compounds. As well, this phenomenon could explain differences in dark toxicity profiles against the two strains as a function of oxygen tension. It is premature to make a definitive statement based on the current set of studies, but work is underway to address the role of efflux activity in PDI in the maintenance and dissemination of important resistant strains of microorganisms in the hospital setting and, increasingly, in the community [42].

The stark potency of the TLD1400 series as PDI agents is not surprising from the point of view of structure-activity relationships. A detailed structural analysis reveals multiple design features that converge to enhance the photodynamic effect for this class of compounds. Briefly, the basic construct of the PS design is a pseudo octahedral coordination sphere provided by three diimine ligands centered on Ru(II). Two identical ancillary ligands (LL = bpy or dmb, Fig. 1) lend stability to the overall complex but also provide handles for fine-tuning properties such as water solubility for drug delivery, lipophilicity for membrane penetration, and electronics for light absorption and photoreactivity. The remaining ligand IP-TT can be considered the coarse control in that its properties impart absolute limits on the magnitude of Type I and Type II photoreactivity the PS provide. IP-TT is a very special motif that incorporates the ideas and principles behind optoelectronic materials [20] derived from oligothiophenes with the right number of thiophene units to bind with high affinity to DNA and other biomolecules. Oligo- and polythiophenes are n-dopable and p-dopable, acting as the perfect electron conduit in either direction, oxidation or reduction [43]. The free carrier phenomenon is widely known in materials chemistry but has not been exploited to its full potential in the photosciences, namely photobiological applications. In the TLD1400 series, the optimal number of thiophenes is that which maintains the sought-after photoredox properties while ensuring processibility. In other words, both solvent-insolubility and photoreactivity increase with increasing number of thiophenes so there is a useful limit or trade-off, and we have found three to be optimal in PDI against *S. aureus* and MRSA. Therefore, the TLD1400 series is based on one IP-TP ligand and two identical ancillary ligands, bpy in the case of TLD1411 and dmb in TLD1433. Incorporating the IP-TT ligand in a Ru(II) coordination complex was strategic for a number of reasons, not least of which is that the overall cationic structure is known to penetrate gram-negative bacterial cell walls with ease, and the visible light absorption by Ru(II) complexes enables the most common light sources to be used with the PS.

Visible light absorption by the TLD1400 series produces excited states that initiate both Type I and Type II photoprocesses. At normal oxygen tension, these PS generate singlet oxygen with 100% efficiency, yet in hypoxic conditions, they display the remarkable ability to switch to Type I behavior owing to the IP-TP unit that can simultaneously act as an excited state oxidant and reductant. In this study, we demonstrate that different ancillary ligands can be combined with IP-TP to give PDI in hypoxia and that this

Please cite this article in press as: Arenas Y, et al. Photodynamic inactivation of *Staphylococcus aureus* and methicillin-resistant *Staphylococcus aureus* with Ru(II)-based type I/type II photosensitizers. Photodiagnosis and Photodynamic Therapy (2013), http://dx.doi.org/10.1016/j.pdpdt.2013.07.001

activity is potent and applicable to MRSA (Fig. 8), a dangerous microbe that adapts to all levels of oxygen. To illustrate, the PDI effect in both TLD1411 and TLD1433 is operative on a sub-micromolar level with light toxicities (log_{10} reductions) of greater than 7 at sub-micromolar concentrations and over 4 as low as 30 nM for TLD1411 against *S. aureus* in hypoxia. A similar effect was found for TLD1433. Against MRSA, log_{10} reductions of 6 were achieved with as low as 600 nM TLD1433 in hypoxia, with the PDI effect in hypoxia being greater than in normoxia at sub-micromolar concentrations. This ability to initiate Type I activity in hypoxia is further supported by the observation that the TLD1400 series exhibits little to no luminescence upon excitation in deoxygenated solution. Therefore, another nonradiative pathway, apart from singlet oxygen sensitization or first-order ROS generation, must be operative in this class of PS. In the present case, two excited PS molecules could generate a charge-transfer pair, consisting of a PS radical anion and a PS radical cation that serve as reactive species. Such radical pairs have been implicated in photobiological damage elsewhere [31]. Details of this photophysical phenomenon are still under investigation as are studies regarding the influence of the ancillary ligand identity on the overall photobiological activities exhibited by the TLD1400 series of PS, in particular toward their application to PDI in gram-negative strains.

Conclusion

There is a recent recognition that Ru(II) complexes might prove useful as PDI agents, particularly for virulent strains of infectious disease, including gram-negative pathogens, owing to their intrinsic cationic charge. However, these PS will continue to suffer from the inability to destroy microbial targets at low oxygen tension, and since precise knowledge of oxygen tension in a wound, for example, is not possible, the best PDI agent will be one that can function regardless of oxygen tension. In this report, we have demonstrated that it is possible to instill Type I activity into a simple mononuclear Ru(II) complex using principles derived from coordination and materials chemistry. This activity was outlined for *S. aureus* and MRSA in hypoxia, and proved to be as effective, or more effective in some cases, than normoxia. Equally important, the TLD1400 series is active at concentrations of over 3 orders of magnitude lower than the gold standard PS MB. This photodynamic potency applies to bacterial cells and cancer cells alike, and therefore, represents a new paradigm for designing Type I PS using Ru(II) that extends to other clinical applications.

References

[1] Acton QA. *Staphylococcus aureus*: advances in research and treatment: 2011 edition: ScholarlyBrief. ScholarlyEditions 2012.
[2] Honeyman A, Friedman H, Bendinelli M. Staphylococcus aureus Infection and Disease. Springer; 2001.
[3] Ouyang F, Bu P, Huang H, Bao S. [Seven kinds of new SCCmec type in Methicillin-resistant *Staphyloccus aureus* and their susceptibility to the antibiotics]. Wei Sheng Wu Xue Bao 2007 Apr;47(2):201–7.
[4] Levy SB, Marshall B. Antibacterial resistance worldwide: causes, challenges and responses. Nature Medicine Dec 2004;10(12 suppl.):S122–9.
[5] O'Riordan K, Akilov OE, Hasan T. The potential for photodynamic therapy in the treatment of localized infections. Photodiagnosis and Photodynamic Therapy 2005 Dec;2(4):247–62.
[6] Tardivo JP, Del Giglio A, de Oliveira CS, Gabrielli DS, Junqueira HC, Tada DB, et al. Methylene blue in photodynamic therapy: from basic mechanisms to clinical applications. Photodiagnosis and Photodynamic Therapy 2005 Sep;2(3):175–91.
[7] Wainwright M. Photodynamic antimicrobial chemotherapy (PACT). Journal of Antimicrobial Chemotherapy 1998 Jul;42(1):13–28.
[8] Kochevar IE, Redmond RW. Photosensitized production of singlet oxygen. Methods in Enzymology 2000;319:20–8.
[9] Paulo J, MS. Photodynamic therapy in the treatment of osteomyelitis. In: Baptista MS, editor. Osteomyelitis. InTech; 2012.
[10] Hamblin MR, Hasan T. Photodynamic therapy: a new antimicrobial approach to infectious disease? Photochemical & Photobiological Sciences 2004 May;3(5):436–50.
[11] Lei W, Zhou Q, Jiang G, Zhang B, Wang X. Photodynamic inactivation of *Escherichia coli* by Ru(II) complexes. Photochemical & Photobiological Sciences 2011 Jun;10(6):887–90.
[12] Kirdis E, Jonsson I-M, Kubica M, Potempa J, Josefsson E, Masalha M, et al. Ribonucleotide reductase class III, an essential enzyme for the anaerobic growth of *Staphylococcus aureus*, is a virulence determinant in septic arthritis. Microbial Pathogenesis 2007 Nov;43(5-6):179–88.
[13] Arenas Y, Mandel A, Lilge L. Kynetic resazurin assay (KRA) for bacterial quantification of foodborne pathogens 2012 Feb, 82252K-82252K.
[14] Jones WEJ, Smith RA, Abramo MT, Williams MD, Van Houten J. Photochemistry of hetero-tris-chelated ruthenium(ii) polypyridine complexes in dichloromethane. Inorganic Chemistry (USA) 1989 Jun;28(12).
[15] Gerhardt P. Methods for General and Molecular Bacteriology Gerhardt. Washington: American Society for Microbiology; 1994.
[16] Lehmann JF, Mercier HPA, Schrobilgen GJ. The chemistry of krypton. Coordination Chemistry Reviews 2002;233-234:1–39.
[17] Rhys Williams Alun T, Winfield Stephen A, Miller James N. Relative fluorescence quantum yields using a computer-controlled luminescence spectrometer analyst 1983;108:1067–71.
[18] Juris A, Balzani V, Barigelletti F, Campagna S, Belser P, Vonzelewsky A. Ru(II) polypyridine complexes: photophysics, photochemistry, eletrochemistry, and chemiluminescence. Coordination Chemistry Reviews 1988;84:85–277.
[19] Chao H, Li R-H, Jiang C-W, Li H, Ji L-N, Li X-Y. Mono-, di- and tetra-nuclear ruthenium(II) complexes containing 2, 2′-p-phenylenebis(imidazo[4,5-f]phenanthroline): synthesis, characterization and third-order non-linear optical properties. Journal of the Chemical Society, Dalton Transactions 2001;12:1920–6.
[20] Batista RMF, Costa SPG, Belsley M, Lodeiro C, Raposo MMM. Synthesis and characterization of novel (oligo)thienyl-imidazo-phenanthrolines as versatile π-conjugated systems for several optical applications. Tetrahedron 2008 Sep;64(39):9230–8.
[21] Balzani V, Juris A. Photochemistry and photophysics of Ru(II)polypyridine complexes in the Bologna group. From early studies to recent developments. Coordination Chemistry Reviews 2001 Jan;211(1):97–115.
[22] Juris A, Balzani V, Barigelletti F, Campagna S, Belser P, von Zelewsky A. Ru(II) polypyridine complexes: photophysics, photochemistry, eletrochemistry, and chemiluminescence. Coordination Chemistry Reviews 1988 Mar;84(0):85–277.
[23] Yao Liu, Richard Hammitt, Lutterman Daniel A, Joyce Lauren E, Thummel Randolph P, Claudia Turro. Ru(II) complexes of new

Please cite this article in press as: Arenas Y, et al. Photodynamic inactivation of *Staphylococcus aureus* and methicillin-resistant *Staphylococcus aureus* with Ru(II)-based type I/type II photosensitizers. Photodiagnosis and Photodynamic Therapy (2013), http://dx.doi.org/10.1016/j.pdpdt.2013.07.001

tridentate ligands: unexpected high yield of sensitized $^1O_2$. Inorganic Chemistry 2009;48(1):375, 2009.

[24] Jacques SL. Laser-tissue interactions. Photochemical, photothermal, and photomechanical. Surgical Clinics of North America 1992 Jun;72(3):531—58.

[25] Castano AP, Demidova TN, Hamblin MR. Mechanisms in photodynamic therapy: part one—photosensitizers, photochemistry and cellular localization. Photodiagnosis and Photodynamic Therapy 2004 Dec;1(4):279—93.

[26] Welch AJ, van Gemert MJC. Optical-Thermal Response of Laser-Irradiated Tissue. 2nd ed. Springer; 2011.

[27] Marchesini R, Bertoni A, Andreola S, Melloni E, Sichirollo AE. Extinction and absorption coefficients and scattering phase functions of human tissues in vitro. Applied Optics 1989 Jun;28(12):2318—24.

[28] Wainwright M, Byrne MN, Gattrell MA. Phenothiazinium-based photobactericidal materials. Journal of Photochemistry and Photobiology B: Biology 2006 Sep;84(3):227—30.

[29] Wainwright M, Phoenix D, Marland J, Wareing DR, Bolton F. A study of photobactericidal activity in the phenothiazinium series. FEMS Immunology and Medical Microbiology 1997 Sep;19(1):75—80.

[30] Ken Kang-Hsin Wang, Finlay Jarod C, Busch Theresa M, Hahn Stephen M, Timothy C. Zhu Explicit dosimetry for photodynamic therapy: macroscopic singlet oxygen modeling. Journal of Biophotonics 2010;3:304—18.

[31] Capella MAM, Capella LSJ. A light in multidrug resistance: photodynamic treatment of multidrug-resistant tumors. Journal of Biomedical Science 2003;10:361—6.

[32] Mendez-Vilas A. Science Against Microbial Pathogens: Communicating Current Research and Technological Advances. Badajoz, Spain: Formatex Research Center; 2011.

[33] Schastak S, Ziganshyna S, Gitter B, Wiedemann P, Claudepierre T. Efficient photodynamic therapy against Gram-positive and Gram-negative bacteria using THPTS, a cationic photosensitizer excited by infrared wavelength. PLoS ONE 2010 Jul;5(7):e11674.

[34] Embleton ML, Nair SP, Cookson BD, Wilson M. Antibody-directed photodynamic therapy of methicillin resistant *Staphylococcus aureus*. Microbial Drug Resistance 2004 Jun;10(2):92—7.

[35] Monika Kossakowska, Joanna Nakonieczna, Anna Kawiak, Julianna Kurlenda, Bielawski Krzysztof P, Mariusz Grinholc. Discovering the mechanisms of strain-dependent response of *Staphylococcus aureus* to photoinactivation: oxidative stress toleration, endogenous porphyrin level and strain's virulence. Photodiagnosis and Photodynamic Therapy 2013.

[36] Maisch T, Bosl C, Szeimies RM, Lehn N, Abels C. Photodynamic effects of novel XF porphyrin derivatives on prokaryotic and eukaryotic cells. Antimicrobial Agents and Chemotherapy 2005;49:1542—52.

[37] Embleton ML, Nair SP, Heywood W, Menon DC, Cookson BD, Wilson M. Development of a novel targeting system for lethal photosensitization of antibiotic-resistant strains of *Staphylococcus aureus*. Antimicrobial Agents and Chemotherapy 2005;49:3690—6.

[38] Szpakowska M, Lasocki K, Grzybowski J, Graczyk A. Photodynamic activity of the haematoporphyrin derivative with rutin and arginine substituents (HpD-Rut(2)-Arg(2)) against *Staphylococcus aureus* and *Pseudomonas aeruginosa*. Pharmacological Research 2001;44:243—7.

[39] Grinholc M, Szramka B, Kurlenda J, Graczyk A, Bielawski KP. Bactericidal effect of photodynamic inactivation against methicillin-resistant and methicillin-susceptible *Staphylococcus aureus* is strain-dependent. Journal of Photochemistry and Photobiology B 2008 Jan 30;90(1):57—63. Epub 2007 Nov 13.

[40] Yang SJ, Bayer AS, Mishra NN, Meehl M, Ledala N, Yeaman MR, et al. The Staphylococcus aureus two-component regulatory system, GraRS, senses and confers resistance to selected cationic antimicrobial peptides. Infection and Immunity 2012 Jan;80(1):74—81.

[41] Mitchell BA, Brown MH, Skurray RA. QacA multidrug efflux pump from *Staphylococcus aureus*: comparative analysis of resistance to diamidines, biguanidines, and guanylhydrazones. Antimicrobial Agents and Chemotherapy 1998 Feb;42(2):475—7.

[42] Costa SS, Ntokou E, Martins A, Viveiros M, Pournaras S, Couto I, et al. Identification of the plasmid-encoded qacA efflux pump gene in meticillin-resistant *Staphylococcus aureus* (MRSA) strain HPV107, a representative of the MRSA Iberian clone. International Journal of Antimicrobial Agents 2010 Dec;36(6):557—61.

[43] Vardeny Z, Ehrenfreund E, Brafman O, Nowak M, Schaffer H, Heeger AJ, et al. Photogeneration of confined soliton pairs (bipolarons) in polythiophene. Physical Review Letters 1986 Feb;56(6):671—4.

Please cite this article in press as: Arenas Y, et al. Photodynamic inactivation of *Staphylococcus aureus* and methicillin-resistant *Staphylococcus aureus* with Ru(II)-based type I/type II photosensitizers. Photodiagnosis and Photodynamic Therapy (2013), http://dx.doi.org/10.1016/j.pdpdt.2013.07.001